Macromolecules
ARTICLE

Macromolecules **2009**, *42*, 8627–8633 **8627**
DOI: 10.1021/ma9019043

Role of Boron in the Polymer Chemistry and Photophysical Properties of Difluoroboron−Dibenzoylmethane Polylactide

Guoqing Zhang, Ruffin E. Evans, Kirsti A. Campbell, and Cassandra L. Fraser*

Department of Chemistry, University of Virginia, Charlottesville, Virginia 22904

Received August 27, 2009; Revised Manuscript Received October 6, 2009

ABSTRACT: Difluoroboron β-diketonate−polymer conjugates have remarkable solid-state luminescent properties that are useful in a variety of fields including multiphoton microscopy, cell biology, and tumor hypoxia imaging. Despite the successful applications of these systems, the role of boron in these polymeric materials has not been thoroughly investigated. Here we explore a boron-free model system with dibenzoylmethane chromophores in poly(lactic acid) (PLA) for comparison. The hydroxyl-functionalized aromatic diketone, dibenzoylmethane (dbmOH), is weakly fluorescent in the solid state and nonfluorescent in solution while its difluoroboron complex (BF_2dbmOH) is highly emissive in both states. Using dbmOH and BF_2dbmOH as initiators, well-defined end-functionalized polylactides, dbmPLA and BF_2dbmPLA, were obtained via tin-catalyzed controlled ring-opening polymerization. Boronation of the dbmOH initiator affects the polymerization kinetics and the photophysical properties of the resulting BF_2dbmPLA material. Both dbmPLA and BF_2dbmPLA are dual emissive in the solid state, exhibiting both fluorescence and room-temperature phosphorescence (RTP), whereas only BF_2dbmPLA is luminescent in solution. These results suggest that boron plays two roles: (1) as a protecting group in the polymerization and (2) as an emission enhancer. Finally, the presence of dual emission for both polymers indicates that it may be the diketone core structure rather than the difluoroboron that is essential for RTP in a rigid PLA matrix.

Introduction

β-Diketones (bdks) are classic ligands in inorganic chemistry for main group, transition metal, and rare earth complexes.[1] The dibenzoylmethane (dbm) family, in particular, has received much attention. In addition to its role as a metal chelator, medical research has found that favorable properties, such as antioxidant, antitumor, anti-inflammatory, and antibacterial effects, are also included in the clinical profiles of dbm derivatives.[2] With extended π conjugation, these compounds show strong UVA (ultraviolet A: 315−400 nm or 3.10−3.94 eV) absorption and are used in sunscreen products.[3] Furthermore, as "light-harvesting antennae", dbm and its derivatives form complexes with variable coordination numbers that exhibit strong luminescence, making them useful in myriad optics-related applications such as OLEDs[4] and solid-state lasing materials.[5]

Polymeric dibenzoylmethane complexes are also known. For example, Kang and Huang[6] described a conjugated copolymer containing fluorene and Eu−dbm complex monomers and found very efficient energy transfer from fluorene to the Eu repeat unit, with the polymer exhibiting almost exclusively narrow red emission from europium. Site-isolated systems reported by our group include europium-centered heteroarm star block copolymers generated from dbm−polylactide and bipyridine−poly(ε-caprolactone) macroligands in a single step.[7] These systems are capable of nanoscale self-assembly.[8] Further investigation of alcohol-functionalized dbm initiators revealed that dbm sites may interfere with tin catalysts during ring-opening polymerization (ROP), slowing the reactions and leading to diminished molecular weight control.[9] In order to achieve higher molecular weight macroligands with low polydispersity indices (PDIs), protecting groups that effectively block the dbm binding site during polymerization were sought. One approach that we have employed previously is to use metal ions as ligand protecting groups.[10,11] For instance, using hydroxyl-functionalized Fe(III) tris(dbm) as the initiator, lactide ROP reactions are faster and more controlled than those with unprotected dbmOH as the initiator.[11]

Initially, we considered boron systems as protecting groups for dbm during macroligand synthesis; however, the optical properties of boron diketonates are also very attractive to incorporate into PLA biomaterials, and these features soon took center stage. The boron diketonate complex, difluoroboron dibenzoylmethane (BF_2dbm), has long been exploited for its photochemical and photophysical attributes. Building upon early work by Morgan and Tunstall[12] and Brown and Bladon,[13] Chow and coworkers discovered that this class of molecules is photoreactive toward a large variety of unsaturated molecule substrates including aromatic compounds,[14] simple olefins,[15] and acrylate derivatives.[16] They investigated the reaction mechanisms concerning the electronic states of the boron complex and the unsaturated substrates, suggesting the formation of ground-state electron donor−acceptor (EDA) pair.[17] This opened new possibilities for organic synthesis via BF_2dbm photochemistry.

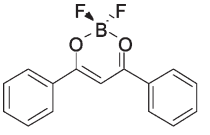

BF_2dbm

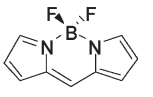

BODIPY Core

Recently, more attention has been paid to the photophysical properties of boron diketone complexes, both in the solid state[18] and in solution[19−21] as new technologies with unprecedented analytical capabilities such as state-of-the-art confocal microscopy in conjunction with multiphoton laser excitation have emerged. These polar dyes possess partial negative charge on BF_2O_2 and partial positive charge on the unsaturated carbon atoms of the

*Corresponding author. E-mail: fraser@virginia.edu.

Published on Web 10/23/2009

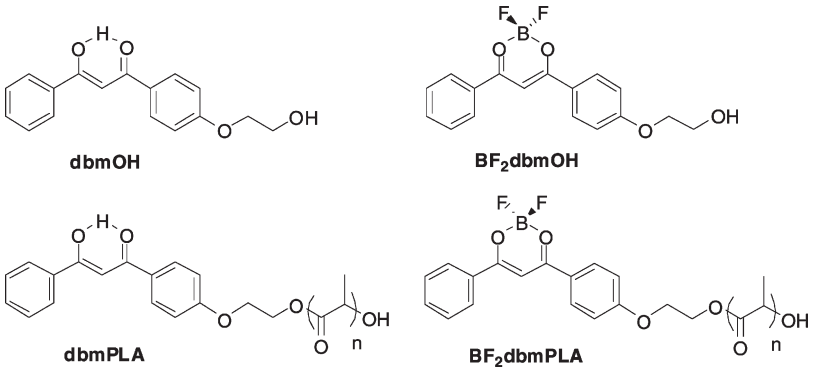

diketonate. They have also found use as electron transport materials for OLEDs[22] and as potent π-acceptor systems with large two-photon[23] cross sections.[24] This attractive feature also made it possible to use BF_2dbmPLA biomaterials fabricated as nanoparticles[25] to image cell trafficking with multiphoton microscopy. Preliminary results indicate that these boron nanoparticles are less prone to photobleaching than other common probes and can be more intensely luminescent than quantum dots.[26]

Although both BF_2dbm and the widely used commercial BODIPY[27] boron difluoride dye series have high fluorescence quantum yields, BF_2dbm and its derivatives are unique in several ways. First, BODIPY dyes tend to self-quench[28] in their aggregate form due to a relatively small Stokes shift; BF_2dbm complexes, in contrast, form emissive excimeric species with red-shifted luminescence at higher concentrations in the solid state and in solution.[29,30] This has led to a simple method for BF_2dbm photoluminescence color tuning, namely, by growing polymers from functionalized BF_2dbm dye initiators (e.g., the biopolymer polylactide, to form BF_2dbmPLA), where the extent of fluorophore−fluorophore (F−F) interactions is easily controlled by the length of the polymer chains which act as separators for the dyes.[31] In addition to dye concentration effects, thermally sensitive delayed fluorescence and oxygen sensitive room temperature phosphorescence (RTP) have also been reported for BF_2dbmPLA.[32] The strong solid-state triplet emission at room temperature is another highlight of BF_2dbm-based systems since very few main group chromophores have been known to possess this property in organic polymers. In comparison, for BODIPY dyes, phosphorescence was observed only by the combination of the dye with a heavy metal complex, and then only at 77 K.[33] BF_2dbmPLA RTP can serve as a powerful tool for quantitative oxygen detection through calibrated RTP spectroscopy, since the large Stokes shift and long-lived emission may minimize the scattered excitation and interference from other short-lived emission. In fact, specially designed dual emissive derivatives exhibiting comparable fluorescence and phosphorescence intensities have been used for *in vivo* ratiometric tumor hypoxia imaging using the oxygen-insensitive fluorescence signal as an internal standard.[34]

Despite many impressive optical properties and the successful application of boron PLA materials in cell and tumor imaging, the influence of the difluoroboron group as a protecting group and fluorophore, compared to dbm, has not been thoroughly investigated. In fact, in organic chemistry, the triplet state of both mono-[35,36] and α-diketones[37,38] has been the focus of research for decades, since carbonyl compounds play a central role in understanding the spectroscopy, photochemistry, and photophysics of polyatomic molecules and their photodissociation. Reports of β-diketones, in contrast, are very sparse,[39] and the influence of polymer matrices on bdk triplet emission is largely unknown. Here we elaborate upon our initial communication[32] and investigate BF_2dbmPLA and dbmPLA chemistry and photophysics in more detail to better understand these unusual multiemissive systems.

Experimental Section

Materials. The initiators dbmOH and BF_2dbmOH were prepared as previously reported.[7,32] 3,6-Dimethyl-1,4-dioxane-2,5-dione (DL-lactide, Aldrich) was recrystallized from ethyl acetate (2×) and stored in a drybox under a nitrogen atmosphere. Tin(II) 2-ethylhexanoate ($Sn(oct)_2$, Spectrum) and all other reagents were used as received. The polymers dbmPLA[7] (**K1**, **K2**) and BF_2dbmPLA[32] (**B1**, **B2**) were prepared as previously reported.

Methods. ^{1}H NMR (300 MHz) spectra were recorded on a Varian UnityInova spectrometer in $CDCl_3$ unless otherwise indicated. Resonances were referenced to the signal for residual protiochloroform at 7.260 ppm. ^{1}H NMR coupling constants are given in hertz. UV−vis spectra were recorded on a Hewlett-Packard 8452A diode-array spectrophotometer in CH_2Cl_2. Molecular weights were determined by two different methods: (1) GPC (THF, 25 °C, 1.0 mL/min) against polystyrene standards using an autosampler (DbmPLA and BF_2dbmPLA molecular weights multiplied by 0.58 correction factor[40]); (2) end-group to polymer integration ratio from ^{1}H NMR spectra (BF_2dbm aromatic vs PLA methine protons). A Polymer Laboratories 5 μm mixed-C guard column and two GPC columns along with Agilent Technologies instrumentation (series 1100 HPLC) were used in GPC analysis.

Steady-state fluorescence emission spectra were recorded on a Horiba Fluorolog-3 model FL3-22 spectrofluorometer (double-grating excitation and double-grating emission monochromators). Phosphorescence spectra were recorded with the same instrument except that a pulsed xenon lamp (λ_{ex} = 369 nm; duration < 1 ms) was used for excitation, and spectra were collected with a 1 ms delay after excitation. Time-correlated single-photon counting (TCSPC) fluorescence lifetime measurements were performed with a NanoLED-370 (369 nm) excitation source and DataStation Hub as the SPC controller. Phosphorescence lifetimes were measured with a 500 ns multichannel scalar card (MCS) excited with a pulsed xenon lamp (λ_{ex}=369 nm; duration < 1 ms). Lifetime data were analyzed with DataStation v2.4 software from Horiba Jobin Yvon.

Polymerization Kinetics. BF_2dbmOH (10.0 mg, 0.030 mmol), lactide (0.865 g, 60 mmol), and $Sn(oct)_2$ (0.24 mg, 0.60 μmol) in hexanes were combined in a sealed round Kontes flask under N_2. The entire bulb of the flask was submerged in a 130 °C oil bath (to prevent the monomer from solidifying on the upper walls of the flask). Aliquots were drawn up into a pipet tip at the specified times, and then the flask was resealed under nitrogen. Samples were analyzed by GPC (method 1, vs polystyrene standards) and ^{1}H NMR spectroscopy (method 2, relative integration). Percent monomer consumption was obtained by comparing the integration of monomer vs (monomer+ polymer) peaks via ^{1}H NMR spectroscopy.

Quantum Yield Measurements. Fluorescence quantum yields, Φ_F, for BF_2dbmPLA in CH_2Cl_2 were calculated versus anthracene in EtOH as a standard as previously described[41] using the following values: Φ_F(anthracene) = 0.27,[42] n_D^{20}(EtOH) = 1.361, n_D^{20}(CH_2Cl_2) = 1.424. Optically dilute CH_2CH_2 solutions of

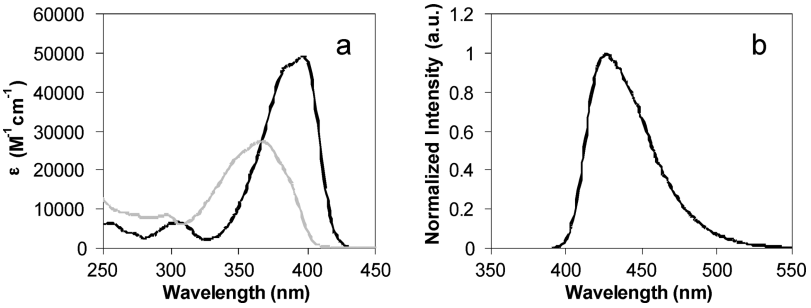

Figure 1. Absorption spectra of (a) dbmOH (gray) and BF_2dbmOH (black) and (b) fluorescence emission of BF_2dbmOH in CH_2Cl_2.

BF_2dbmPLA and EtOH solutions of the anthracene standard were prepared in 1 cm path length quartz cuvettes, and absorbances ($A < 0.1$) were recorded using a Hewlett-Packard 8452A UV/vis spectrometer. Steady-state emission spectra were obtained on a Horiba Fluorolog-3 model FL3-22 spectrofluorometer ($\lambda_{ex} = 350$ nm; emission integration range: 365−700 nm).

Results and Discussion

Synthesis and Optical Properties of Diketone and Boron Initiators. DbmOH, the ligand precursor for the BF_2dbmOH initiator, was prepared as previously reported by Bender et al.[7] with the following modifications. After purification of the crude product by column chromatography, the solid was dissolved in hot 60:40 hexanes/EtOAc, and bright yellow needles formed immediately upon sonification. The boron initiator, BF_2dbmOH, was synthesized from $BF_3 \cdot OEt_2$ and dbmOH in CH_2Cl_2 with stirring for an hour at 60 °C as reported.[32] The crude product, a dark yellow foam, is best recrystallized from acetone/hexanes, but other solvent systems such as EtOAc/hexanes are also possible. The final product was obtained as bright yellow needlelike crystals. Boronation was verified by ^{1}H NMR spectroscopy ($CDCl_3$). The dbmOH diketone tautomer methylene ($COCH_2CO$) peak at 4.60 ppm and the enol H peak at 16.99 ppm were no longer evident in the difluoroboron product. Instead, the enol tautomer OH−C(Ar)=C*H* proton shifted from 6.81 to 7.12 ppm.

Although dbmOH is weakly fluorescent in the solid state upon UV excitation, in comparison, the BF_2dbmOH solid exhibits intense yellowish-green emission probably due to stronger intermolecular interactions (e.g., dipole−dipole, arene−arene, B−F···H−O− hydrogen bonds).[18,43] The physical properties of dbmOH and BF_2dbmOH were investigated in solution. Although BF_2dbmOH is soluble in most organic solvents such as acetone, THF, CH_2Cl_2, and EtOAc, its solubility is significantly reduced compared to dbmOH perhaps due to an increased dipole moment (e.g., BF_2dbm, 6.7 D[13] compared to 2.7 D for dbm[44]). In CH_2Cl_2, dbmOH and BF_2dbmOH exhibit $\pi-\pi^*$[17,39,45] transitions at 354 nm ($\varepsilon = 27\,700$ M^{-1} cm^{-1}) and 397 nm ($\varepsilon = 53\,000$ M^{-1} cm^{-1}), respectively. Addition of difluoroboron to dbmOH, however, results in an almost 2-fold increase in extinction coefficient, suggesting stronger $\pi-\pi^*$ character for BF_2dbmOH (Figure 1). The CH_2Cl_2 solution of dbmOH is not fluorescent at room temperature while BF_2dbmOH exhibits intense blue emission. The fluorescence lifetime of BF_2dbmOH in CH_2Cl_2 was measured to be 1.95 ns with single-exponential decay. A very high fluorescence quantum yield is also noted ($\Phi_F = 0.95$). Solution fluorescence data show that dbmOH is nonemissive, but addition of the $-BF_2$ electron accepting group[46] results in moderately fluorescent BF_2dbm[19] ($\Phi_F = 0.20$). With an extra electron donating group such as −OR, the compound BF_2dbmOMe ($\Phi_F = 0.85$)[19] and BF_2dbmOH have remarkably enhanced quantum yields. This implies that the efficient fluorescence of BF_2dbmOH may arise from an intramolecular donor-to-acceptor charge transfer (CT) state, where a better donor−acceptor structure (RO− and BF_2O_2−) efficiently enhances the radiative decay compared to alkoxy and boron-free dbmOH. This stronger D−A nature points to the possibility of a larger two-photon absorption (TPA) cross section compared to a weaker D−A molecule[47] such as BF_2dbm. The measurement was therefore performed, and the TPA cross section for BF_2dbmOH in acetone is ∼37 GM.[48] That is, by addition of an electron-donating group, the TPA cross section of the molecule has increased more than 10-fold versus BF_2dbm (2−3 GM).[19]

Table 1. Representative Reaction Kinetics for dbmPLA and BF_2dbmPLA[a]

dbmPLA[b]			BF_2dbmPLA[b]		
time (h)	M_n[c] (kDa)	PDI[d]	time (h)	M_n[c] (kDa)	PDI[d]
3.0	3100	1.08	0.33	3100	1.08
6.0	4800	1.08	1.5	11400	1.06
9.8	5800	1.12	4	19800	1.14
43.0	15800	1.23	7	22300	1.30

[a] Data derived from sample aliquots taken during polymerization. [b] Initiator:lactide:Sn(oct)$_2$ = 1:200:1/50. [c] GPC number-average molecular weight detected by refractive index in THF applying 0.58 correction factor against polystyrene standards.[40] [d] PDI = polydispersity index.

Polymer Synthesis. Solvent-free bulk polymerization was conducted at 130 °C because the melting point for DL-lactide is 126 °C, and the lowest reaction temperature possible can help to minimize dye degradation and other side reactions. Previously, we have reported the synthesis of dbmOH[7] and the polymerization of DL-lactide with dbmOH to prepare dbmPLA macroligands for metal complexation.[49] Without the BF_2 functionality, the dbmOH initiator has relatively slow polymerization kinetics due to likely interactions between the diketone and the Sn(oct)$_2$ catalyst. Typically, dbmPLA with a molecular weight of ∼3000 Da was obtained after ∼3 h at 130 °C (Table 1). In comparison, with the same catalyst loading (1:50 catalyst:initiator) and at the same temperature, but with boron occupying the diketone binding site, BF_2dbmOH is capable of a generating a polymer with a much higher molecular weight at reduced reaction time. With typical 1:200 initiator to monomer loading, well-defined BF_2dbmPLA polymers with M_n up to 20 kDa can be obtained after a few hours. Beyond that, the M_n starts to plateau, but the PDI continues to increase and the reaction loses control. Higher temperatures result in faster polymerization and higher MW polymers under the same conditions (monomer loading and reaction time), but the M_n obtained after a given reaction time lacks consistency from run to run (Table 2). Given that many desirable optical properties are observed for polymers in the 3−20 kDa range,[31] 130 °C remains the optimal temperature for accurate MW targeting.

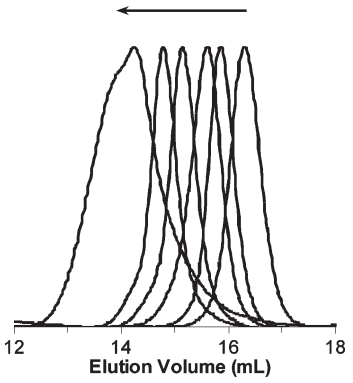

Figure 2. GPC traces of purified preparative scale BF_2dbmPLA of different molecular weights in THF (increasing M_n indicated by the arrow: 2.5, 4.6, 6.2, 9.5, 13.2, and 20.2 kDa; PDIs: 1.10, 1.10, 1.15, 1.12, 1.16, and 1.63).

Table 2. Representative Reaction Kinetics for Polymerization of DL-Lactide Initiated by BF_2dbmOH at Different Temperatures[a]

	130 °C		145 °C		160 °C	
time (min)	M_n[b] (kDa)	PDI	M_n[b] (kDa)	PDI	M_n[b] (kDa)	PDI
10	1000	1.07	2500	1.08	5100	1.10
20	2600	1.10	5400	1.13	13900	1.10
40	5100	1.09	10800	1.10	25200	1.15
60	7000	1.10	15100	1.11	30200	1.18
90	10600	1.08	20600	1.12	31700	1.23

[a] Data derived from sample aliquots taken during polymerization. BF_2dbmOH:lactide:Sn(oct)$_2$ = 1:500:1/50. [b] GPC number-average molecular weight detected by refractive index in THF solvent, applying 0.58 correction factor[40] against polystyrene standards.

Purified polymers can be easily obtained by dissolving the reaction mixture in CH_2Cl_2 and then precipitating the solution twice in cold MeOH and then once in room temperature hexanes. Despite the fact that Lewis bases such as MeOH can solvolyze BF_2dbmOH over time to generate the parent diketone dbmOH,[50] the polymer extinction coefficients were the same after five precipitations in MeOH (to remove all traces of unreacted monomer) as for two precipitations. Also, no enol peak is observed at 16.9 ppm, as is typically observed for ^{1}H NMR spectra ($CDCl_3$) of dbmPLA and dye degraded samples. This is because either the deboronation in MeOH takes a long time[50] or that the presence of the PLA chain has effectively protected the boron center from MeOH solvolysis during the precipitation. Narrow and symmetric GPC traces verified that well-defined BF_2dbmPLA[32] samples were obtained (Figure 2).

Solution Optical Properties. The absorption spectra of dbmPLA (353 nm) and BF_2dbmPLA (396 nm) polymers in CH_2Cl_2 are very similar to those of the dbmOH (354 nm) and BF_2dbmOH (397 nm) initiators, as expected. This indicates that PLA has a minimal effect on the electronic transitions of the chromophores in solution. DbmPLA polymers remain nonfluorescent in solution, and the fluorescence spectrum of BF_2dbmPLA in CH_2Cl_2 again corresponds well with that of BF_2dbmOH except that the former has a slightly broadened emission, possibly from more vibrational and rotational freedom for BF_2dbmPLA. In spite of the subtle variations in fluorescence quantum yields for BF_2dbmPLA polymers of different MWs (~0.75−0.90, essentially within experimental error), all the boron diketone polymers, regardless of their MWs, exhibit the same spectra (~434 nm) with lifetimes (~1.9 ns) that fit to single-exponential decay in CH_2Cl_2 solution.

Solid-State Optical Properties. In contrast to the optical properties of BF_2dbmPLA in solution, where the polymer molecular weight barely affects the optical properties, BF_2dbmPLA has more interesting and complex solid-state luminescence. First, the fluorescence is highly MW dependent, especially in the 3−10 kDa range where greenish-yellow (3 kDa) to blue (10 kDa) fluorescence is observed in both powder and film forms.[31] We have ascribed this phenomenon to stronger and weaker fluorophore−fluorophore interactions between the dye molecules in the polymers of different molecular weights (i.e., different dye loading and matrix dielectric due to variable concentrations of the polar dye).[31] Second, in the absence of oxygen, unusual room-temperature phosphorescence (RTP)[32] was observed for all the BF_2dbmPLA polymers.

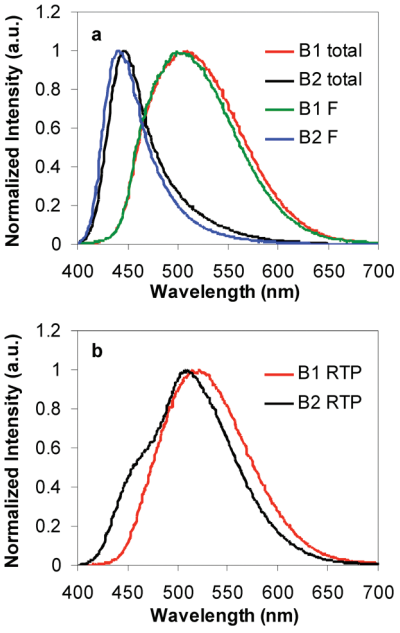

Figure 3. Steady-state spectra (a) under N_2 (total: total emission) and air (F: fluorescence) and delayed spectra (RTP) (b) under N_2 of BF_2dbmPLA polymers at room temperature excited at 369 nm. Delayed spectra were collected 2 ms after the excitation pulse ceased.

Figure 3 shows the emission spectra of a 3 kDa (**B1**) and 26 kDa (**B2**) BF_2dbmPLA polymers in the solid state. As expected, both samples have fluorescence, RTP, and delayed fluorescence in the emission spectra under N_2. The fluorescent emission maxima for **B1** and **B2** are 499 and 440 nm under air, respectively, and are consistently red-shifted under N_2 (509 and 447 nm) probably due to the contribution from the RTP. The fluorescence lifetimes measured for **B1** and **B2** are 23.54 and 3.00 ns (Table 3), which, together with the significant spectral red shift and broadening for **B1**, have been previously described as a result of F−F interactions in the excited state. It was assumed that stronger F−F interactions significantly reduce the energies of singlet excited states for polymers with much higher dye loadings such as **B1**. Thus, the maxima for fluorescence (499 nm) and delayed spectra (522 nm) are very close for **B1** (23 nm, similar effects are also seen in acridine yellow in trehalose glass[51]) but are quite different for **B2** (440 and 507 nm, 67 nm difference). Delayed emission lifetimes (Table 3) also support this assumption since **B2** has a substantially longer lived emission (426 ms) compared to **B1** (125 ms) perhaps due to a much larger singlet−triplet (ST) energy splitting and a smaller probability of thermal repopulation of the short-lived singlet excited state from the triplet state.

Initially, these features were anticipated to be unique to the BF_2dbm chromophore in a PLA matrix. But surprisingly, the

Table 3. Luminescence Emission Data for BF_2dbmPLA (B1 and B2) and dbmPLA (K1 and K2) in the Solid State at Room Temperature under N_2

	M_n GPC[a] (kDa)	PDI[b]	λ_F (nm)[c]	τ_F (ns)[d]	$\lambda_{em,RTP}$ (nm)[e]	τ_{RTP} (ms)[h]
B1	2.1	1.09	499	23.54	522[f]	125[f]
B2	20.9	1.24	440	3.00	507[f]	426[f]
K1	3.0	1.15	437	0.86	505[g]	81[g]
K2	12.1	1.29	435	0.66	500[g]	94[g]

[a] Number-average molecular weight detected by refractive index in THF solvent, applying 0.58 correction factor[40] against polystyrene standards. [b] PDI = polydispersity index. [c] Steady-state fluorescence spectra under air. Excitation source: 369 nm xenon lamp. [d] Pre-exponential weighted fluorescence lifetime.[52] Excitation source: 369 nm light-emitting diode; fluorescence lifetime fit to triple-exponential decay. [e] Delayed emission spectra under N_2 (Δt = 2 ms). Excitation source: xenon flash lamp. [f] λ_{ex} = 396 nm. Excitation source: xenon flash lamp. [g] λ_{ex} = 353 nm. Excitation source: xenon flash lamp. [h] Pre-exponential weighted RTP lifetime. Excitation source: xenon flash lamp; RTP lifetime fit to triple-exponential decay.

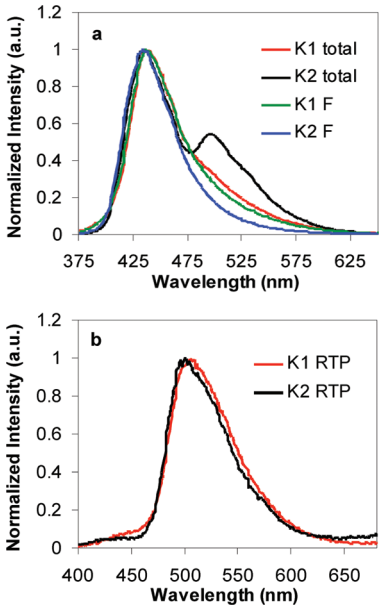

Figure 4. Steady-state spectra (a) under N_2 (total: total emission) and air (F: fluorescence) and delayed spectra (RTP) (b) under N_2 of dbmPLA polymers at room temperature excited at 369 nm. Delayed spectra were collected 2 ms after the excitation pulse ceased.

diketone polymers dbmPLA of different MWs exhibited the same emission patterns under N_2; namely, both blue fluorescence and green long-lived RTP were observed. The steady-state and delayed spectra of dbmPLA with two different MWs (**K1** and **K2**) under N_2 are shown in Figure 4. Similar to BF_2dbmPLA, dbmPLA also exhibits MW-dependent emission but to a much lesser extent. First, although the high molecular weight dbmPLA, **K2**, has a slightly narrower steady-state emission spectrum, the emission maximum (435 nm) barely shows any difference in comparison to **K1** (437 nm). Second, the RTP spectra of both **K1** and **K2** are essentially identical and lack significant delayed fluorescence shoulders. As proposed, the MW-dependent color shift in the solid state for BF_2dbmPLA may arise from F−F interactions in the excited state. The largely unchanged spectra for dbmPLA polymers indicate that the excited state dipole for dbm is weaker, as expected. The steady-state spectra, especially for **K2** under N_2, however show a higher RTP/fluorescence intensity ratio in comparison with **B1** and **B2**. Similar emission maxima for **K1** and **K2** fluorescence and RTP along

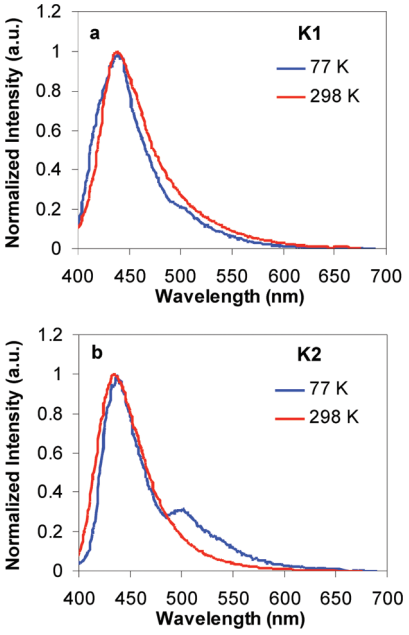

Figure 5. Steady-state emission spectra of dbmPLA polymers (a) **K1** and (b) **K2** at 77 and 298 K.

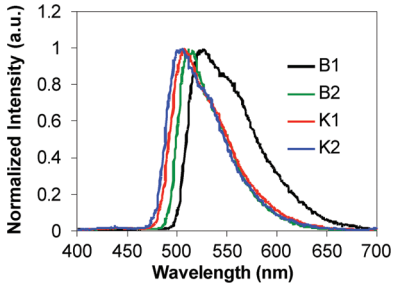

Figure 6. Delayed emission spectra (Δt = 2 ms) of BF_2dbmPLA (**B1** and **B2**) and dbmPLA (**K1** and **K2**) polymers at 77 K (BF_2dbmPLA: λ_{ex} = 396 nm; dbmPLA: λ_{ex} = 353 nm).

with similar RTP lifetimes suggest the singlet−triplet energy splitting is comparable for **K1** and **K2** at room temperature. Therefore, the differences in the triplet decay could be due to competition with the nonradiative process associated with matrix rigidity or excimeric species formation. However, low-temperature experiments do not support the former possibility. Figure 5 shows that the emission maxima for both **K1** and **K2** barely change with the temperature variation, and it is likely that excited-state interactions are responsible for the diminished RTP shoulder for **K1**.

Low-Temperature Phosphorescence. Low-temperature measurements are also useful for estimating the intrinsic triplet lifetime with and without boron chelation. Thus, the delayed spectra of dbmPLA and BF_2dbmPLA polymers were measured at low temperature where thermal repopulation is largely inhibited. At 77 K, the delayed fluorescence peaks for BF_2-dbmPLA are negligible for all polymers (Figure 6), and the phosphorescence lifetimes for **B1** and **B2** are 1.75 and 1.72 s, respectively. The decay profiles compared to those at room temperature are much less complicated. Both lifetimes can be fit well to double-exponential decay with $\kappa^2 < 1.1$. In addition, the pre-exponential weighted lifetimes are very close to those obtained with single-exponential fittings. For dbmPLA, however, the lifetimes are much shorter (**K1**: 191 ms; **K2**: 192 ms) and the decays are nonexponential ($\kappa^2 > 1.2$ fit to triple-exponential decay). This again may be because dbmPLA has

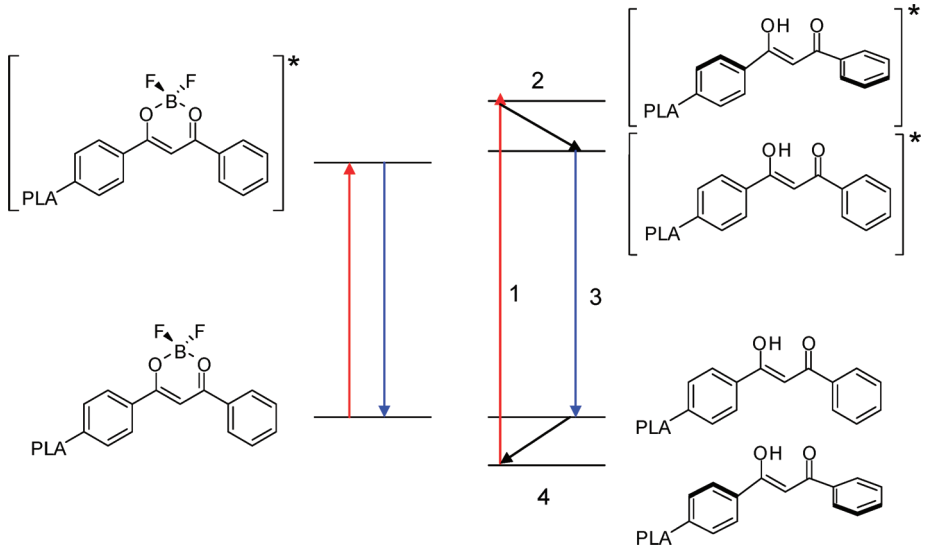

Figure 7. Simplified Jablonski diagrams illustrating the proposed emission mechanism for BF_2dbmPLA and dbmPLA. BF_2dbmPLA (left): roughly planar and no significant conformational difference between the ground and excited states. DbmPLA (right): nonplanar in the ground state and upon excitation (1) the Franck−Condon state relaxes to a more planar excited state (2). After emitting a photon (3), the more stable ground state (4) is achieved.

an intramolecular hydrogen bond, and such structures tend to undergo very rapid nonradiative decay.[53] In addition, dbmPLA can have both diketone and enol forms, where the tautomerization may complicate the decay.

Proposed Emission Mechanisms. The absorption maxima of dbmPLA (**K1** and **K2**) in CH_2Cl_2 are 353 nm, and their emissions in the solid state are peaked around 436 nm. The surprisingly large Stokes shift may be explained by conformational changes in the excited-state structure. A study of the dbm crystal structure by XRD[54] revealed that the diketone is nonplanar in the ground state. Specifically, the planes of the phenyl rings are tilted −3.8° and +16.9° with respect to the enol ring. The dramatically red-shifted emission spectrum suggests that following the Franck−Condon state the relaxed excited state might be more planar than the ground state. In comparison, the XRD crystal structure of BF_2dbm is more planar (+3.1° and +3.5°)[55] in the ground state, and that may explain the relatively smaller Stokes shift. In this case, less molecular reorganization is required during electronic transitions. Planar excited states with similar π conjugation lengths could also help explain the very similar F and RTP maxima for dbmPLA (**K2**) and BF_2dbmPLA (**B2**).

Many mono- and diketones exhibit phosphorescence at low and room temperature, and their mechanisms have been thoroughly studied. Monoketones, such as acetophenone, typically have structured and blue-shifted (386 nm, 77 K) phosphorescence compared to diketones containing vicinal carbonyls, the emission spectra of which are usually structureless perhaps due to carbonyl−carbonyl interactions (e.g., benzil phosphorescence: 532 nm, 77 K).[56] In the case of dbmPLA, the phosphorescence does not present any defined structure, and the triplet energy level (500 nm) lies between those of acetophenone and benzil. For dbmPLA, however, it is hard to attribute the structureless phosphorescence to interactions between the two carbonyl triplet states, given both enol and keto forms. Wright et al.[39] performed low-temperature phosphorescent measurements under conditions that distinguished diketone and enolic contributions. They attributed the structured high-energy shoulder (390 nm) to the diketone tautomer and the less structured peak at 490 nm to the enolic dbm triplet emission. On the basis of this precedence, dbmPLA RTP likely arises from a planar enolic structure. The hypothesis is illustrated in Figure 7.

Conclusion

In summary, we prepared the primary alcohol-functionalized dibenzoylmethane-based diketone initiator dbmOH and difluoroboron diketonate initiator BF_2dbmOH for solvent-free ring-opening polymerization (ROP) of DL-lactide and obtained reasonably well-defined dbmPLA and BF_2dbmPLA polymers. The role of boron as a protecting group in lactide ROP chemistry and in the photophysics of the polymers was investigated. Boronated BF_2dbmOH, compared to diketone dbmOH, serves as a more efficient ROP initiator for lactide due to the boron protection of the diketone site which prevents dbm complexation with tin(II). As a result, the ROP rate with BF_2dbmOH as an initiator is an order of magnitude faster that with dbmOH under the same conditions.

Photophysical studies on the polymers dbmPLA and BF_2dbmPLA show that in solution dbmPLA is nonfluorescent whereas BF_2dbmPLA is intensely fluorescent. In the solid state under N_2, however, both dbmPLA and BF_2dbmPLA exhibited fluorescence and unusual room temperature phosphorescence. Previous results showed that the fluorescence of BF_2dbmPLA has strong polymer molecular weight dependency. In comparison, here it is shown that the weakly fluorescent dbmPLA has a much smaller color tuning range, suggesting weaker excited state interactions among the fluorophores. These observations are consistent with the assumption that while boron has immensely enhanced the excited state dipoles of strongly fluorescent BF_2dbmPLA, the RTP of both dbmPLA and BF_2dbmPLA are perhaps intrinsic to the diketone structure. In addition, we propose that dbmPLA has a very different molecular configuration between the ground and the excited states in order to account for its large Stokes shift (~83 nm). The fact that more polar BF_2dbmPLA has a smaller Stokes shift suggests that with boron rigidifying the chromophore both ground- and excited-state BF_2dbmPLA have more planar structures. Photophysical studies of dbmPLA and BF_2dbmPLA have important implications for room temperature phosphorimetry. Surprisingly similar solid-state emission phenomena for the diketone and its difluoroboron complex suggest that both luminophore classes may serve as starting points for sensor design.

Acknowledgment. We thank the National Science Foundation (CHE 0718879) for support for this work and Dr. Jessica L. Gorczynski and Mr. Jianbin Chen for their pioneering work with dbmPLA and BF_2dbmPLA materials.

References and Notes

(1) (a) Vigato, P. A.; Peruzzo, V.; Tamburini, S. *Coord. Chem. Rev.* **2009**, *253*, 1099–1201. (b) Darr, J. A.; Poliakoff, M. *Chem. Rev.* **1999**, *99*, 495–542. (c) Koepf-Maier, P.; Koepf, H. *Chem. Rev.* **1987**, *87*, 1137–1152.

(2) (a) Jackson, K. M.; Frazier, M. C.; Harris, W. B. *Anticancer Res.* **2007**, *27*, 1483–1488. (b) Lin, C.-C.; Tsai, Y.-L.; Huang, M.-T.; Lu, Y.-P.; Ho, C.-T.; Tseng, S.-F.; Teng, S.-C. *Carcinogenesis* **2006**, *27*, 131–136. (c) Singletary, K.; MacDonald, C.; Iovinelli, M.; Fischer, C.; Wallig, M. *Carcinogenesis* **1998**, *19*, 1036–1043.

(3) (a) Huong, S. P.; Rocher, E.; Fourneron, J.-D.; Charles, L.; Monnier, V.; Bun, H.; Andrieu, V. *J. Photochem. Photobiol. A: Chem.* **2008**, *196*, 106–112. (b) Scalia, S.; Villani, S.; Scatturin, A.; Vandelli, M. A.; Forni, F. *Int. J. Pharm.* **1998**, *175*, 205–213.

(4) Kido, J.; Okamoto, Y. *Chem. Rev.* **2002**, *102*, 2357–2368.

(5) Kuriki, K.; Koike, Y.; Okamoto, Y. *Chem. Rev.* **2002**, *102*, 2347–2356.

(6) Ling, Q. D.; Kang, E. T.; Neoh, K. G.; Huang, W. *Macromolecules* **2003**, *36*, 6995–7003.

(7) Bender, J. L.; Corbin, P. S.; Fraser, C. L.; Metcalf, D. H.; Richardson, F. S.; Thomas, E. L.; Urbas, A. M. *J. Am. Chem. Soc.* **2002**, *124*, 8526–8527.

(8) Manners, I. *Science* **2001**, *294*, 1664–1666.

(9) Bender, J. L.; Shen, Q.-D.; Fraser, C. L. *Tetrahedron* **2004**, *60*, 7277–7285.

(10) McAlvin, J. E.; Scott, S. B.; Fraser, C. L. *Macromolecules* **2000**, *33*, 6953–6964.

(11) Gorczynski, J. L.; Chen, J.; Fraser, C. L. *J. Am. Chem. Soc.* **2005**, *127*, 14956–14957.

(12) Morgan, G. T.; Tunstall, R. B. *J. Chem. Soc.* **1924**, *125*, 1963–1967.

(13) Brown, N. M. D.; Bladon, P. *J. Chem. Soc. A* **1969**, 526–532.

(14) Chow, Y. L.; Ouyang, X. *Can. J. Chem.* **1991**, *69*, 423–431.

(15) Chow, Y. L.; Heng, X. *Can. J. Chem.* **1991**, *69*, 1575–1583.

(16) Chow, Y. L.; Wang, S.; Cheng, X. *Can. J. Chem.* **1993**, *71*, 846–854.

(17) Chow, Y. L.; Wang, S.; Johansson, C. I.; Liu, Z. *J. Am. Chem. Soc.* **1996**, *118*, 11725–11732.

(18) (a) Mirochnik, A.; Fedorenko, E.; Kuryavyi, V.; Bukvetskii, B.; Karasev, V. *J. Fluoresc.* **2006**, *16*, 279–286. (b) Mirochnik, A.; Fedorenko, E.; Gizzatulina, D.; Karasev, V. *Russ. J. Phys. Chem. A* **2007**, *81*, 1880–1883.

(19) Cogné-Laage, E.; Allemand, J.-F.; Ruel, O.; Baudin, J.-B.; Croquette, V.; Blanchard-Desce, M.; Jullien, L. *Chem.—Eur. J.* **2004**, *10*, 1445–1455.

(20) Nagata, Y.; Otaka, H.; Chujo, Y. *Macromolecules* **2008**, *41*, 737–740.

(21) Nagai, A.; Kodado, K.; Nagata, Y.; Chujo, Y. *Macromolecules* **2008**, *41*, 8295–8298.

(22) Domercq, B.; Grasso, C.; Maldonado, J.-L.; Halik, M.; Barlow, S.; Marder, R.; Kippelen, B. *J. Phys. Chem. B* **2004**, *108*, 8647–8651.

(23) Albota, M.; Beljonne, D.; Brédas, J.-L.; Ehrlich, J. E.; Fu, J.-Y.; Heikal, A. A.; Hess, S. E.; Kogej, T.; Levin, M. D.; Marder, S. R.; McCord-Maughon, D.; Perry, J. W.; Rockel, H.; Rumi, M.; Subramaniam, G.; Webb, W. W.; Wu, X.-L.; Xu, C. *Science* **1998**, *281*, 1653–1656.

(24) Halik, M.; Wenseleers, W.; Grasso, C.; Stellacci, F.; Zojer, E.; Barlow, S.; Brédas, J.-L.; Perry, J. W.; Marder, S. R. *Chem. Commun.* **2003**, 1490–1491.

(25) Pfister, A.; Zhang, G.; Zareno, J.; Horwitz, A. F.; Fraser, C. L. *ACS Nano* **2008**, *2*, 1252–1258.

(26) Contreras, J.; Xie, J.; Pei, H.; Chen, Y. J.; Zhang, G.; Fraser, C. L.; Hamm-Alvarez, S. F., submitted.

(27) (a) Loudet, A.; Burgess, K. *Chem. Rev.* **2007**, *107*, 4891–4932. (b) Ulrich, G.; Ziessel, R.; Harriman, A. *Angew. Chem., Int. Ed.* **2008**, *47*, 1184–1201.

(28) Ozdemir, T.; Atilgan, S.; Kutuk, I.; Yildirim, L. T.; Tulek, A.; Bayindir, M.; Akkaya, E. U. *Org. Lett.* **2009**, *11*, 2105–2107.

(29) Mirochnik, A. G.; Gukhman, E. V.; Zhihareva, P. A.; Karasev, V. E. *Spectrosc. Lett.* **2002**, *35*, 309–315.

(30) Chow, Y. L.; Cheng, X.; Johansson, C. I. *J. Photochem. Photobiol. A: Chem.* **1991**, *57*, 247–255.

(31) Zhang, G.; Kooi, S. E.; Demas, J. N.; Fraser, C. L. *Adv. Mater.* **2008**, *20*, 2099–2104.

(32) Zhang, G.; Chen, J.; Payne, S. J.; Kooi, S. E.; Demas, J. N.; Fraser, C. L. *J. Am. Chem. Soc.* **2007**, *129*, 8942–8943.

(33) (a) Galletta, M.; Campagna, S.; Quesada, M.; Ulrich, G.; Ziessel, R. *Chem. Commun.* **2005**, *33*, 4222–4224. (b) Nastasi, F.; Puntoriero, F.; Campagna, S.; Diring, S.; Ziessel, R. *Phys. Chem. Chem. Phys.* **2008**, *10*, 3982–3986.

(34) Zhang, G.; Palmer, G. M.; Dewhirst, M. W.; Fraser, C. L. *Nat. Mater.* **2009**, *8*, 747–751.

(35) Fang, W.-H. *Acc. Chem. Res.* **2008**, *41*, 452–457.

(36) (a) Lamola, A. A. *J. Chem. Phys.* **1967**, *47*, 4810–4816. (b) Koyanagi, M.; Zwarich, R. J.; Goodman, L. *J. Chem. Phys.* **1972**, *56*, 3044–3060.

(37) Rubin, M. B.; Gleiter, R. *Chem. Rev.* **2000**, *100*, 1121−1164 (section VIII).

(38) (a) Almgren, M. *Photochem. Photobiol.* **1969**, *9*, 1–6. (b) Speiser, S.; Hassoon, S.; Rubin, M. B. *J. Phys. Chem.* **1986**, *90*, 5085–5089.

(39) Gacoin, P. *J. Chem. Phys.* **1972**, *57*, 1418–1425.

(40) (a) Baran, J.; Duda, A.; Kowalski, A.; Szymanski, R.; Penczek, S. *Macromol. Rapid Commun.* **1997**, *18*, 325–333. (b) Save, M.; Schappacher, M.; Soum, A. *Macromol. Chem. Phys.* **2002**, *203*, 889–899.

(41) Demas, J. N.; Crosby, G. A. *J. Phys. Chem.* **1971**, *75*, 991−1024 (section II.C.2, eq 16).

(42) Dawson, W. R.; Windsor, M. W. *J. Phys. Chem.* **1968**, *72*, 3251–3260.

(43) Zhang, G.; Sabat, M.; Fraser, C. L. Unpublished results.

(44) Saad, G. R.; Naoum, M. M.; Rizk, H. A. *Can. J. Chem.* **1989**, *67*, 284–288.

(45) Morita, H.; Nakanishi, H. *Bull. Chem. Soc. Jpn.* **1981**, *54*, 378–386.

(46) Fabian, J.; Hartmann, H. *J. Phys. Org. Chem.* **2004**, *17*, 359–369.

(47) Rumi, M.; Ehrlich, J. E.; Heikal, A. A.; Perry, J. W.; Barlow, S.; Hu, Z.; McCord-Maughon, D.; Röckel, H.; Thayumanavan, S.; Marder, S. R.; Beljonne, D.; Brédas, J.-L. *J. Am. Chem. Soc.* **2000**, *122*, 9500–9510.

(48) Jhaveri, S.; Ober, C. K.; Zipfel, W. R.; Zhang, G.; Fraser, C. L. Unpublished results.

(49) Gorczynski, J. L. Ph.D. Thesis, University of Virginia, **2005**.

(50) Mackay, S. C.; Preston, P. N.; Will, S. G.; Morley, J. O. *J. Chem. Soc., Chem. Commun.* **1982**, *7*, 395–396.

(51) Fister, J. C.III; Harris, J. M.; Rank, D.; Wacholtz, W. *J. Chem. Educ.* **1997**, *74*, 1208–1212.

(52) Carraway, E. R.; Demas, J. N.; DeGraff, B. A.; Bacon, J. R. *Anal. Chem.* **2002**, *63*, 337–342.

(53) Lamola, A. A.; Sharp, L. J. *J. Phys. Chem.* **1966**, *70*, 2634–2638.

(54) Williams, D. E. *Acta Crystallogr.* **1966**, *21*, 340–349.

(55) Mirochnik, A. G.; Bukvetskii, B. V.; Gukhman, E. V.; Zhikhareva, P. A.; Karasev, V. E. *Russ. Chem. Bull.* **2001**, *50*, 1612–1615.

(56) Morantz, D. J.; Wright, A. J. C. *J. Chem. Phys.* **1971**, *54*, 692–697.